

# Hydrothermal synthesis of nanocrystalline BaSnO<sub>3</sub> using a SnO<sub>2</sub>·xH<sub>2</sub>O sol

Wensheng Lu\*, Helmut Schmidt

*Leibniz-Institut fuer Neue Materialien gem. GmbH, Im Stadtwald, Gebaeude 43A, D-66123 Saarbruecken, Germany*

## Abstract

A BaSnO<sub>3</sub> powder with a crystallite size of 27.6 nm has been prepared through a hydrothermal reaction of a peptised SnO<sub>2</sub>·xH<sub>2</sub>O and Ba(OH)<sub>2</sub> at 250 °C and the following crystallization of this hydrothermal product at 330 °C. The peptisation of the SnO<sub>2</sub>·xH<sub>2</sub>O gel is dependent on the pH value. Through peptisation the mean particle size of SnO<sub>2</sub>·xH<sub>2</sub>O in the aqueous solution has been decreased by a factor of 100 to 8 nm. A limited agglomeration in the sol-prepared powder has been observed under the microscope. The structure evolution and crystallisation behaviours of the sol-prepared powders were investigated by TG-DTA, IR and XRD. The BaSn(OH)<sub>6</sub> phase in the as-prepared powder transforms into an amorphous phase at 260 °C, from which the BaSnO<sub>3</sub> particles nucleate and grow with an increase in temperature. The single-phase BaSnO<sub>3</sub> powder has been obtained at a temperature as low as 330 °C. This sol-prepared powder is more sinter-reactive than the gel-prepared powder and can be sintered to a ceramic with 90.7% of the theoretic density.

**Keywords** Powders-chemical; Preparation; Electron microscopy; X-ray methods; Perovskites; Sensors; BaSnO<sub>3</sub>

## 1. Introduction

As a perovskite-structured ceramic BaSnO<sub>3</sub> is becoming more and more important in material technology because of its characteristic dielectric properties. It has been used to prepare thermally stable capacitors<sup>1,2</sup> and to fabricate ceramic boundary layer capacitors when combined with BaTiO<sub>3</sub>.<sup>3,4</sup> In recent years BaSnO<sub>3</sub> has been found to be a very promising sensor material and therefore received much attention. In pure as well as doped forms stannates have been employed as sensor materials for a lot of gases, including CO, H<sub>2</sub>, Cl<sub>2</sub>, NO<sub>x</sub> and humidity.<sup>5–9</sup> BaSnO<sub>3</sub> has also been used in the preparation of multifunctional temperature–humidity–gas sensors in combining with BaTiO<sub>3</sub>.<sup>10</sup>

The BaSnO<sub>3</sub> powder is conventionally prepared by ceramic solid reaction through sintering BaCO<sub>3</sub> and SnO<sub>2</sub> at a high temperature ranging from 1200 to 1400 °C.<sup>11,12</sup> A preparation of the BaSnO<sub>3</sub> powder by heating a coprecipitate of hydrated barium stannates at 1000 °C was reported by Coffen.<sup>13</sup> However, the often simultaneously formed

solid barium tin hydroxide made it difficult to obtain the phase-pure BaSnO<sub>3</sub> at high temperatures.<sup>14</sup> A modified sol–gel method<sup>15</sup> was used to prepare BaSnO<sub>3</sub> powder from tin chloride and barium carbonate by adding a chelating agent such as citric acid, the synthesised aqueous gel had nevertheless to be calcined at 600 °C for 5 h and then annealed at 1000 °C for 17 h to convert into a BaSnO<sub>3</sub> powder. Azad and Hon<sup>16</sup> tried to prepare BaSnO<sub>3</sub> by the self-heat-sustained route from metallic tin powder and anhydrous Ba(NO<sub>3</sub>)<sub>2</sub>. However, a high calcination temperature more than 1200 °C is necessary to obtain phase-pure BaSnO<sub>3</sub>. A polymerised complex method<sup>17</sup> was also taken to prepare BaSnO<sub>3</sub> powder, in which a barium tin citric acid complex precursor was converted into aggregated BaSnO<sub>3</sub> by treating at a temperature range of 600–900 °C, but it is difficult to remove the trace amounts of BaCO<sub>3</sub> and SnO<sub>2</sub> even at 900 °C.

Compared with the above described synthesis methods, the hydrothermal synthesis route reported by Kutty and Vivekanadan<sup>18</sup> for preparing BaSnO<sub>3</sub> powders shows its advantage in the low synthesis temperature. Fine BaSnO<sub>3</sub> powders can be prepared by this method starting from a SnO<sub>2</sub>·xH<sub>2</sub>O gel at a temperature as low as 260 °C. However, the particle size of the obtained powder is in the micrometer

\* Corresponding author.

E-mail address lu@inm-gmbh.de (W. Lu).

region (0.2–0.6  $\mu\text{m}$ ). A low specific surface area resulting from such large particles (the specific surface area which was not referred in the literature 18 could be estimated to be 1.38–4.14  $\text{m}^2/\text{g}$  according to the particle size without consideration of the aggregation) is not beneficial to the sensitivity of the sensing device. It is known that the detection of gas in the sensors containing  $\text{BaSnO}_3$  is performed by measurement of the changes in electrical properties such as conductivity. The changes are induced in the semiconducting  $\text{BaSnO}_3$  following the adsorption of some gases on the solid surface. The mechanism of the gas sensitivity of this semiconducting oxide is a surface reaction process.<sup>8,9</sup> Thus a large surface area of the oxide powder is of importance to its characteristic sensor properties. For obtaining a large surface area the main task is to decrease the degree of aggregation between the particles. As well as  $\text{SnO}_2 \cdot x\text{H}_2\text{O}$  is concerned, its agglomerates can be redispersed into a colloidal solution through peptisation<sup>19</sup> (the process of converting a gel to a sol). Thus, the aim of this paper is to prepare a perovskite  $\text{BaSnO}_3$  powder with a large specific surface area through peptisation of the  $\text{SnO}_2 \cdot x\text{H}_2\text{O}$  gel. The thermal behaviours, the structure evolution, the crystallisation behaviours and the sintering properties of the obtained stannate powder are also reported here.

## 2. Experimental procedure

The precursor  $\text{SnO}_2 \cdot x\text{H}_2\text{O}$  gel was synthesised according to the literature<sup>20</sup> by adding 2.5 M ammonia solution to 1 M  $\text{SnCl}_4$  solution at an ice bath. To remove the  $\text{Cl}^-$  ions the gel was washed with distilled water several times until its electric conductivity was less than 50  $\mu\text{S}/\text{cm}$ . For obtaining a sol the washed gel was diluted to 0.3 M, in which 25% ammonia solution as a peptisator was added slowly under stirring. The amount of the ammonia solution was controlled by measuring the pH value of the mixture. The tin oxide hydrate sol was then mixed with 0.2 M  $\text{Ba}(\text{OH})_2$  solution by using argon as the protecting gas. The mixture was thereafter charged in an 1 l teflon-lined autoclave (step motor, Berghof) and treated under hydrothermal conditions at 250 °C for 6 h. The product was taken out at room temperature and washed with distilled water until its pH value was near 7. The powder was then calcined in an oven at temperatures ranging from 260 to 330 °C for a defined time.

In the experiment the pH value was measured by a pH meter (pH 535, WTW) with an integrated temperature sensor. The crystalline phase of the powder was analysed with a D500 model diffractometer (Siemens, radiation Cu K $\alpha$ 1) operating at 40 kV. The crystallite size was calculated from Scherrer equation.<sup>21</sup> The thermal behaviours of the samples were analysed through thermogravimetric analysis and differential thermal analysis (TG-DTA: STA501, Baer). The infrared spectra of the samples treated at different temperatures were recorded with a Fourier transform infrared spectrometer (IFS 25v, Bruker) to analyse the structure

evolution. The structure and morphology of powders were studied with a high resolution transmission electron microscope (HR-TEM: CM 200 FEG, Philips). The specific surface area of the powders were characterised with a BET gas adsorption analyser (ASAP 2400, Micrometrics). The particle size distribution of the tin oxide hydrate was measured by a ultrafine particle analyser (UPA 400, Leeds Northrup). The linear shrinkage of pellet samples which were uniaxially pressed to a dimension of ca.  $\varnothing$  5 mm  $\times$  5 mm under a pressure of 400 MPa was measured with a differential dilatometer (Linseis). The pellet was heated to 1650 °C at a rate of 10 °C/min in air atmosphere. Samples for sintering were pellets with a dimension of about  $\varnothing$  10 mm  $\times$  1 mm which were formed by a cold isostatic pressure of 400 MPa. The green body was heated to 1600 °C at 10 °C/min and soaked for 4 h. The bulk density of the sintering ceramic was measured by the Archimedes method with water as the immersing media. The surface of the polished sintered samples was investigated with the scanning electron microscope (JSM 6400F, JEOL) using 10 kV accelerating voltage.

## 3. Results and discussion

The  $\text{SnO}_2 \cdot x\text{H}_2\text{O}$  gel suspended in water can be peptised by using ammonia solution as the peptising agent. It was found that the peptising effect of ammonia to the  $\text{SnO}_2 \cdot x\text{H}_2\text{O}$  gel depends on the pH value. The suspensions with a pH from 6.8 to 7.2 are milky white, which cannot change into transparent sols even after being aged for a long time. At a pH value between 8.3 and 9.8 the suspensions convert into transparent sols through peptisation within 2–12 h. The higher the pH value, the less time is necessary for the peptisation.

The particle diameter distribution of the samples at different pH values are shown in Fig. 1. It can be seen from Fig. 1a that the particle diameter of samples at pH 6.8 and pH 7.2 distributes in a range from 0.5 to 1.5  $\mu\text{m}$  while at pH 8.3 to pH 9.8 in a range less than 20 nm. Fig. 1b shows the dependence of the mean particle diameter ( $d_{50}$ -value of the volume distribution) of the samples on the pH-value. A sharp decrease of the  $d_{50}$ -value can be observed at pH between 7.2 and 8.2, where the  $d_{50}$  is decreased from about 0.8  $\mu\text{m}$  by a factor of 100 to 8 nm.

From this it can be concluded that a tin oxide hydrate sol will be formed from the tin oxide hydrate gel through peptisation as the pH-value exceeds 8.3. In the experiments the pH value was controlled at pH 9.3 by adding the ammonia solution for obtaining a stable  $\text{SnO}_2 \cdot x\text{H}_2\text{O}$  sol within 6 h. It should be pointed out that the  $\text{SnO}_2 \cdot x\text{H}_2\text{O}$  gels used for peptisation was freshly synthesised because an aged gel will lose its activity through losing the hydrated water.<sup>22</sup> For example, a aged gel (three days) could not be peptised.

The powders synthesised from the  $\text{SnO}_2 \cdot x\text{H}_2\text{O}$  gel or the  $\text{SnO}_2 \cdot x\text{H}_2\text{O}$  sol by hydrothermal reaction with the  $\text{Ba}(\text{OH})_2$  solution at 250 °C for 6 h consist of  $\text{BaSn}(\text{OH})_6$  (this will

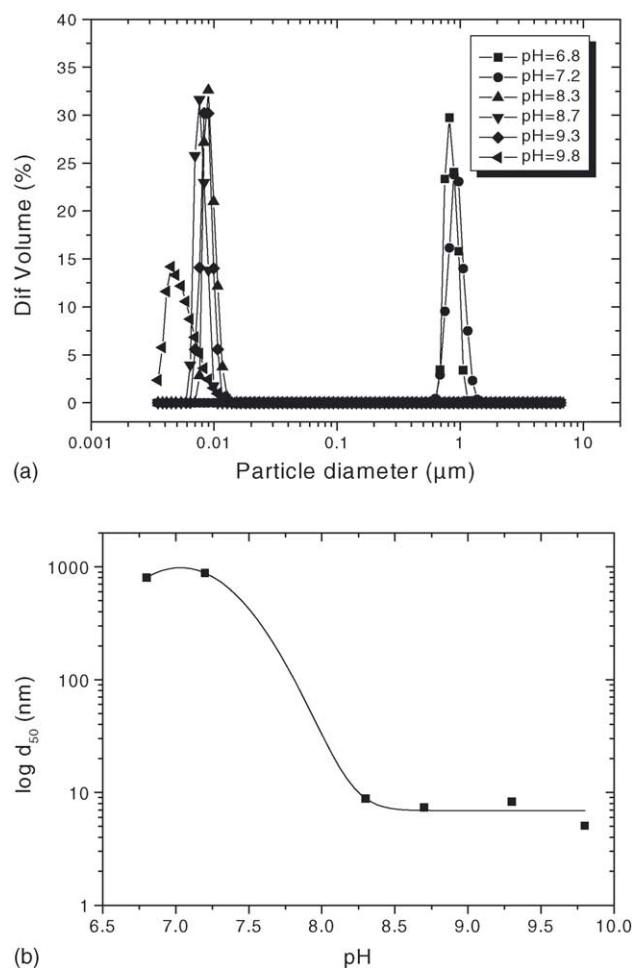


Fig. 1. (a) Particle diameter contribution, (b) mean particle diameter  $d_{50}$  of the tin oxide hydrate peptised at different pH.

be discussed later). Figs. 2 and 3 show the HR-TEM micrographs of the powders derived from the  $\text{SnO}_2 \cdot x\text{H}_2\text{O}$  gel and the  $\text{SnO}_2 \cdot x\text{H}_2\text{O}$  sol, respectively (the marked particles are processed with Fourier-transformation, Fourier-filtering and morphologic operation). Fig. 2a indicates the high agglomeration state of  $\text{BaSn}(\text{OH})_6$ , not even a single particle is recognisable. Fig. 2b shows that these agglomerates consist of many overlapped crystallites with a diameter of 10–50 nm. In contrast to this,  $\text{BaSn}(\text{OH})_6$  derived from the  $\text{SnO}_2 \cdot x\text{H}_2\text{O}$  sol is constituted of much smaller clusters ranging from 20 to 200 nm (Fig. 3a). The clusters connect with each other loosely. It is shown from the structure image (Fig. 3b) that the size of the nanocrystallites is about 3 nm. Therefore, peptisation is helpful to minimise the agglomeration of the particles and lower the particle size of the powders.

Fig. 4 shows the TG-DTA curve of the power prepared from the sol. Two endothermic peaks located at 270 and 330 °C can be found in the DTA curve, which corresponds to the dehydration and dehydroxylation process of the sol-prepared powder. In accordance with the DTA curve, two main weight loss stages, namely from room temperature to 300 °C and from 300 to 400 °C, can be found in

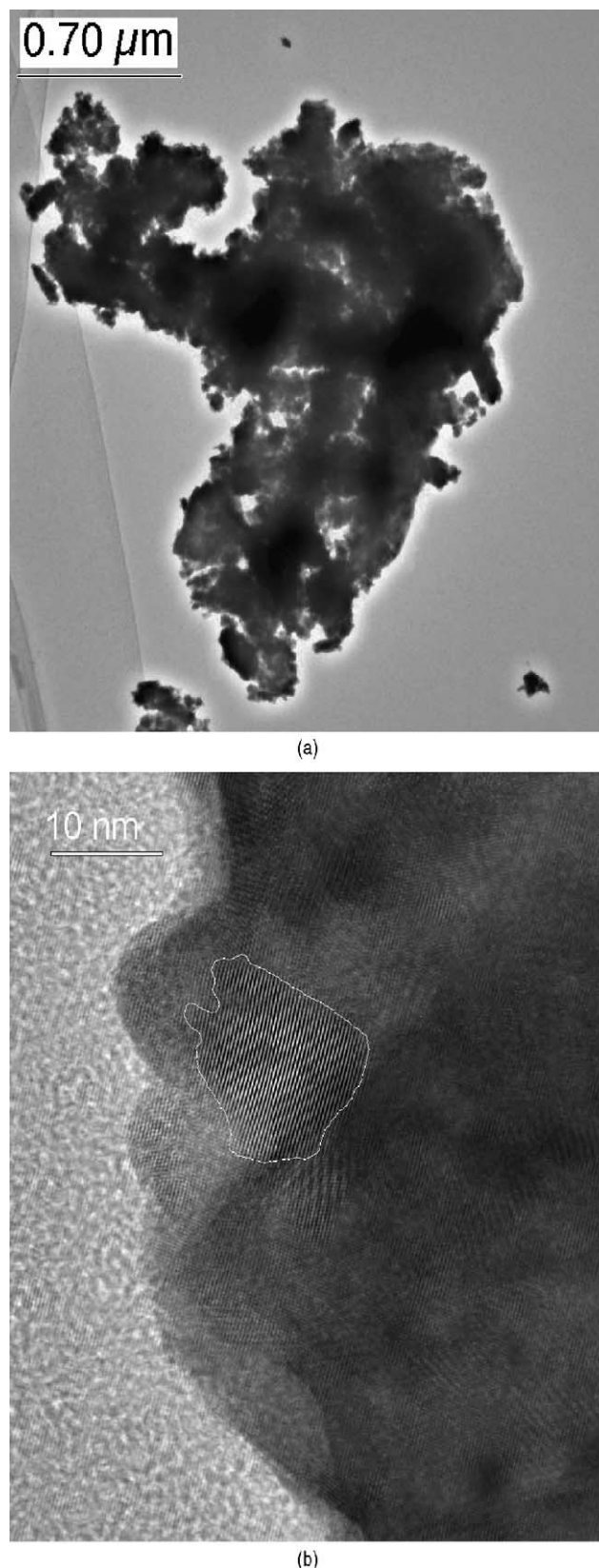


Fig. 2. HR-TEM micrographs of the gel-prepared powder of  $\text{BaSn}(\text{OH})_6$ : (a) diffraction contrast imaging, (b) structure imaging.  $\text{BaSn}(\text{OH})_6$  was hydrothermally synthesised from the  $\text{SnO}_2 \cdot x\text{H}_2\text{O}$  gel and  $\text{Ba}(\text{OH})_2$  at 250 °C for 6 h.



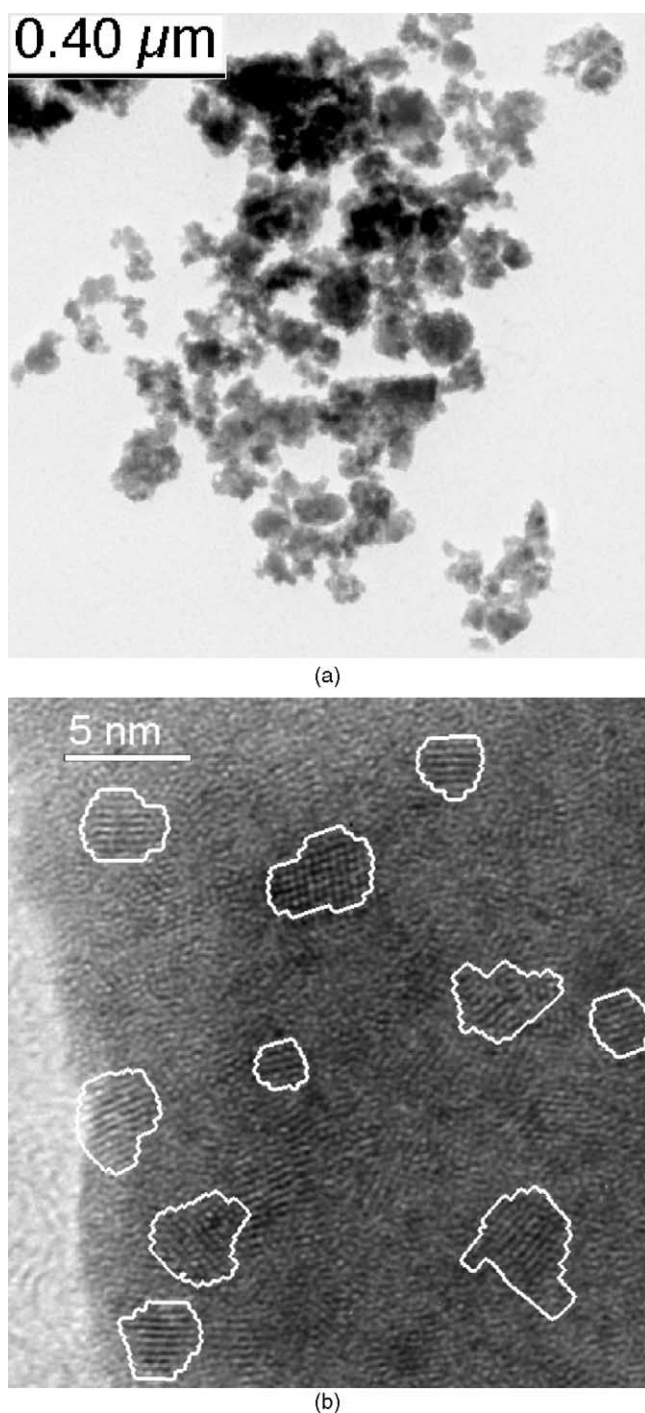


Fig. 3. HR-TEM micrographs of the sol-prepared powder of  $\text{BaSn}(\text{OH})_6$ : (a) diffraction contrast imaging, (b) structure imaging.  $\text{BaSn}(\text{OH})_6$  was hydrothermally synthesised from the  $\text{SnO}_2 \cdot x\text{H}_2\text{O}$  sol and  $\text{Ba}(\text{OH})_2$  at  $250^\circ\text{C}$  for 6 h.

the TG curve. The weight loss in the first stage and the second stage is 8.6 and 3.7 wt.%, respectively. Thereafter the weight decreases slowly from  $400$  to  $800^\circ\text{C}$  (1.6 wt.%). Above  $800^\circ\text{C}$  little weight change can be observed. Calculated from the TG results, the constitution of the as-prepared powder can be noted as  $\text{BaSnO}_3 \cdot 2.73\text{H}_2\text{O}$ , it becomes

$\text{BaSnO}_3 \cdot 1.04\text{H}_2\text{O}$  and  $\text{BaSnO}_3 \cdot 0.31\text{H}_2\text{O}$  at  $300$  and  $400^\circ\text{C}$ , respectively.

The structure evolution of the sol-prepared powder calcined at different temperatures was investigated with the help of FTIR spectra. The FTIR spectra of the samples are shown in Fig. 5. It can be seen that the five-set peaks around  $500\text{ cm}^{-1}$  signalling the Sn-OH group in the as-prepared powder round off at  $260^\circ\text{C}$  after 4 h of calcination. At the same time a peak localising at  $630\text{ cm}^{-1}$  representing the octahedron structure  $[\text{SnO}_6]$  appears in the spectrum. The Sn-OH peak disappears completely and the intensity of the  $[\text{SnO}_6]$  peak increases at  $330^\circ\text{C}$  after 4 h of calcination. It can therefore be concluded that the dehydroxylation takes place at  $260^\circ\text{C}$ . As a consequence, the structure rearranges and the octahedron structure  $[\text{SnO}_6]$  begins to form. At  $330^\circ\text{C}$  the structure rearrangement finishes and therefore no Sn-OH groups can be found in the spectrum.

To study the crystallisation behaviour of the sol-prepared powder, the powder was calcined at different temperatures ranging from  $260$  to  $330^\circ\text{C}$  for definite time. Fig. 6 shows the XRD patterns of these samples. The as-prepared powder consists of  $\text{BaSn}(\text{OH})_6$ . It transforms into amorphous after being calcined at  $260^\circ\text{C}$  for 4 h.  $\text{BaSnO}_3$  nucleates from the amorphous phase and grows either by increasing the temperature or extending the treatment time, the effect of the temperature is nevertheless more obvious. The transformation of  $\text{BaSn}(\text{OH})_6$  to  $\text{BaSnO}_3$  ends at  $330^\circ\text{C}$  and a single-phase  $\text{BaSnO}_3$  powder was obtained at  $330^\circ\text{C}$  after 4 h of calcination. The crystallite size of the  $\text{BaSnO}_3$  calculated according to Scherrer equation is  $27.6\text{ nm}$ .

By comparison, the crystallisation process of the gel-prepared powder was investigated with XRD and the results are illustrated in Fig. 7. The as-prepared powder also consists of  $\text{BaSn}(\text{OH})_6$ . It transforms into amorphous after calcining at  $260^\circ\text{C}$  for 0.25 h. By extending the time to 1 h, a  $\text{BaSnO}_3$  phase appears. The conversion of the amorphous phase into perovskite-type  $\text{BaSnO}_3$  accomplishes after 4 h of calcination at  $260^\circ\text{C}$ . Thus, the single-phase  $\text{BaSnO}_3$  can be prepared at  $260^\circ\text{C}$  from the gel-prepared powder. However, even at a lower calcining temperature of  $260^\circ\text{C}$  (4 h) the crystallite size of the gel-prepared  $\text{BaSnO}_3$  is  $33.0\text{ nm}$  and larger than that of the  $\text{BaSnO}_3$  powder obtained by calcining the sol-prepared  $\text{BaSn}(\text{OH})_6$  at  $330^\circ\text{C}$  for 4 h.

The BET specific surface area of the  $\text{BaSnO}_3$  powder by calcining the sol-prepared  $\text{BaSn}(\text{OH})_6$  at  $330^\circ\text{C}$  for 4 h is  $23.5\text{ m}^2/\text{g}$  while that from the gel-prepared powder at  $260^\circ\text{C}/4\text{ h}$  is only  $5.3\text{ m}^2/\text{g}$ . The obvious increase in specific surface area through peptising the gel can be attributed to the reduction in aggregation between the particles and the decrease in particle size of  $\text{SnO}_2 \cdot x\text{H}_2\text{O}$ .

The shrinkage behaviour of sol- and gel-prepared  $\text{BaSnO}_3$  was studied by means of dilatometry. The green densities of uniaxially pressed sol- and gel-prepared samples ( $400\text{ MPa}$ ) are 47.8 and 45.0% of the theoretic density of  $\text{BaSnO}_3$  ( $7.24\text{ g/cm}^3$ ), respectively. Fig. 8 shows their shrinkage curves. For the sample derived from the gel, its

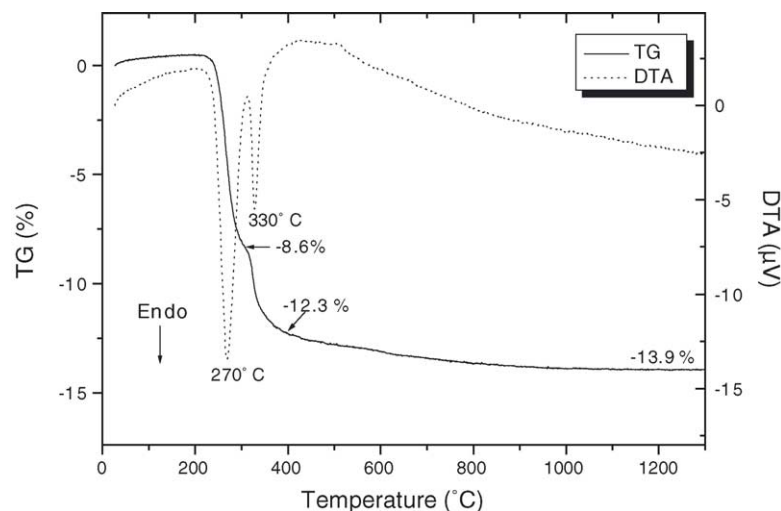


Fig. 4. TG-DTA curve of the sol-prepared powder of  $\text{BaSn(OH)}_6$ . The powder was hydrothermally synthesised from the  $\text{SnO}_2 \cdot x\text{H}_2\text{O}$  sol and  $\text{Ba(OH)}_2$  at  $250^\circ\text{C}$  for 6 h. The heating rate is  $10^\circ\text{C/min}$ .

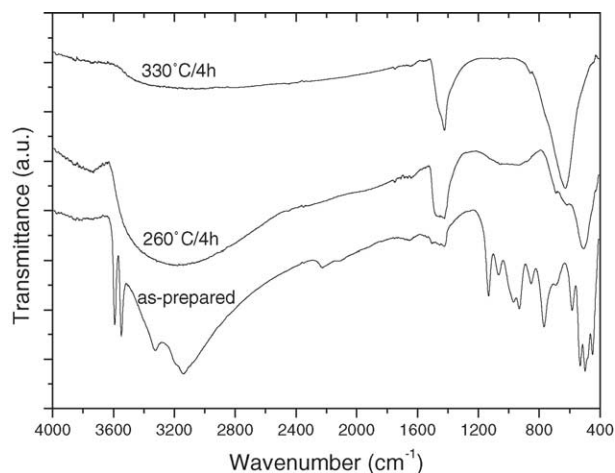


Fig. 5. FTIR spectra of the sol-prepared powder calcined at various temperatures for 4 h. The powder was hydrothermally synthesised from the  $\text{SnO}_2 \cdot x\text{H}_2\text{O}$  sol and  $\text{Ba(OH)}_2$  at  $250^\circ\text{C}$  for 6 h.

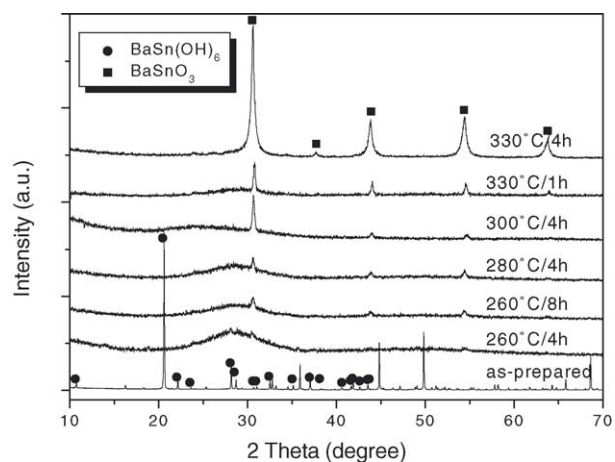


Fig. 6. XRD patterns of the sol-prepared powder calcined at various temperatures and times. The as-prepared powder was hydrothermally synthesised from the  $\text{SnO}_2 \cdot x\text{H}_2\text{O}$  sol and  $\text{Ba(OH)}_2$  at  $250^\circ\text{C}$  for 6 h.

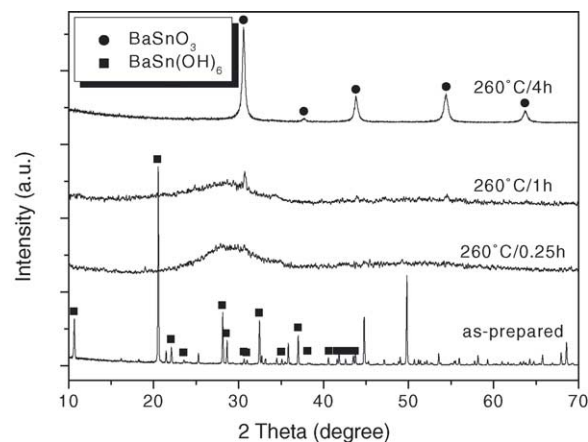


Fig. 7. XRD patterns of the gel-prepared powder calcined at  $260^\circ\text{C}$  for different time. The as-prepared powder was hydrothermally synthesised from the  $\text{SnO}_2 \cdot x\text{H}_2\text{O}$  gel and  $\text{Ba(OH)}_2$  at  $250^\circ\text{C}$  for 6 h.

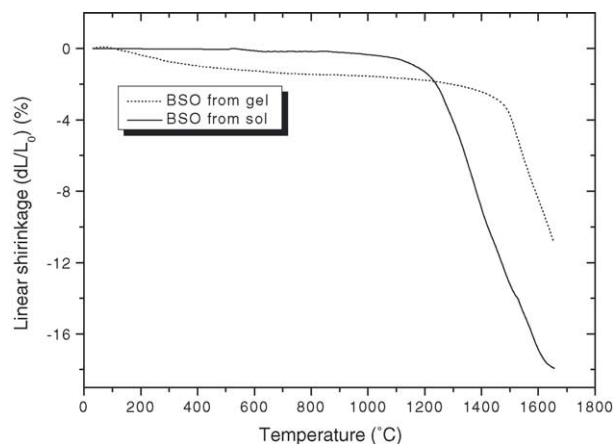


Fig. 8. Dilatometry curves of  $\text{BaSnO}_3$  (BSO) obtained by calcining the gel-prepared  $\text{BaSn(OH)}_6$  powder at  $260^\circ\text{C}$  for 4 h and that obtained by calcining the sol-prepared  $\text{BaSn(OH)}_6$  at  $330^\circ\text{C}$  for 4 h. Heating rate:  $10^\circ\text{C/min}$ .

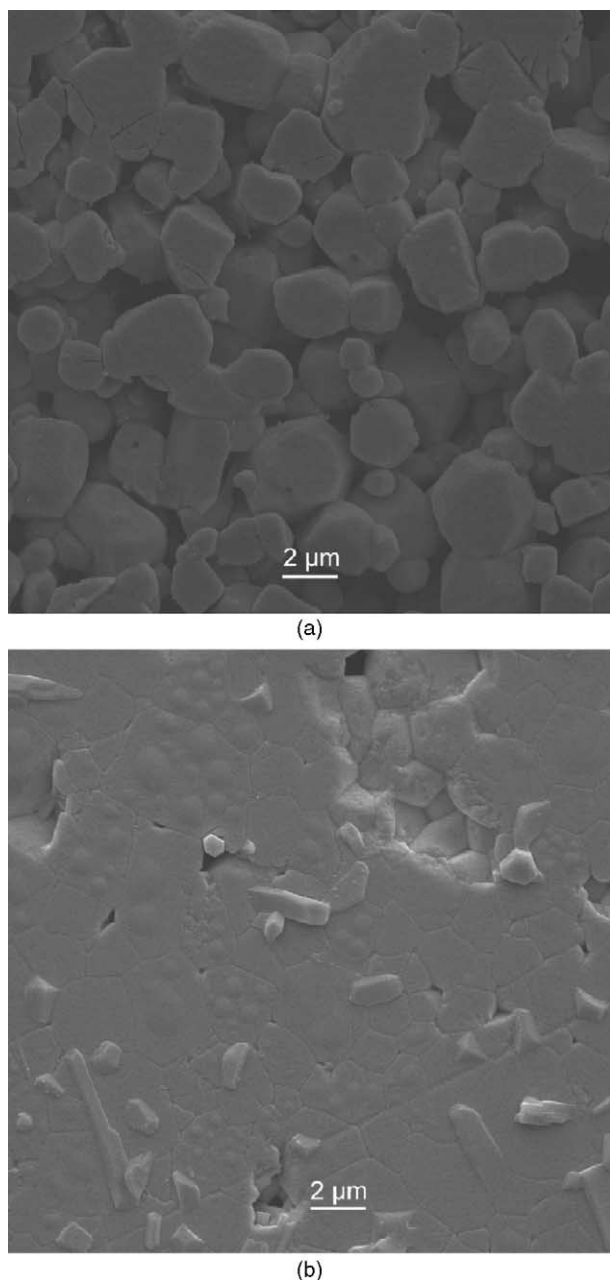


Fig. 9. SEM micrographs of  $\text{BaSnO}_3$  powders sintered at  $1600^\circ\text{C}$  for 4 h: (a) gel-prepared powder calcined at  $260^\circ\text{C}$  for 4 h, (b) sol-prepared powder calcined at  $330^\circ\text{C}$  for 4 h.

sintering begins at  $1450^\circ\text{C}$  and a shrinkage of only 10.2% is reached at  $1650^\circ\text{C}$ . The upper limit of the temperature of equipment is  $1650^\circ\text{C}$  where the sintering process of the sol-prepared sample is not ended. In contrast to that, the onset of the sintering temperature of the sample derived from the sol is lowered to  $1200^\circ\text{C}$  and its shrinkage reaches 17.9% at  $1650^\circ\text{C}$ . Judging from the flattening of the curve near  $1650^\circ\text{C}$ , it can be said that the sintering process of this sample is almost complete. It therefore can be concluded that the sample derived from the sol is more sinter-active. The increase of the sinter-activity can be attributed to

smaller particles and the larger surface area which is the driving force of the sintering process.

$\text{BaSnO}_3$  pellets formed under a cold isostatic pressure of 400 MPa were sintered at the same temperature of  $1600^\circ\text{C}$  for 4 h for comparison. Using the gel-prepared powder a bulk density of  $5.47\text{ g/cm}^3$  (75.6% of the theoretic density) resulted while using the sol-prepared powder a bulk density of  $6.57\text{ g/cm}^3$  (90.7% of the theoretic density) could be obtained. Fig. 9a and b shows the microstructure of the polished surface of two samples sintered at  $1600^\circ\text{C}$  for 4 h, starting from the gel- and sol-prepared  $\text{BaSnO}_3$  powders, respectively. For the gel-prepared sample (Fig. 9a), the powder did not densified enough so that the pores still connect with each other. In contrast to this, the sol-prepared ceramic (Fig. 9b) are much more dense and only some isolated pores can be observed. At a sintering temperature of  $1600^\circ\text{C}$ , the grain size of both samples is in the  $\mu\text{m}$ -region. Generally the grains of the sol-prepared sample are finer than those of the gel-prepared sample, but some grains as large as  $2\text{--}3\mu\text{m}$  in the former can also be observed. The large grain size in the  $\text{BaSnO}_3$  ceramic can be attributed to the grain growth at the high sintering temperature.

#### 4. Summary

In this study, a single-phase nano-crystalline  $\text{BaSnO}_3$  powder with a specific surface area as large as  $23.5\text{ m}^2/\text{g}$  has been prepared through the hydrothermal reaction between tin oxide hydrate sol and  $\text{Ba}(\text{OH})_2$  at  $260^\circ\text{C}$  and the following crystallisation of the resulted powder at  $330^\circ\text{C}$ . The tin oxide hydrate sol was obtained by peptising the tin oxide hydrate gel through adding the ammonia solution. The peptisation is dependent on the pH value and the particle sizes of the tin oxide hydrate sol are in the range less than 20 nm. Through peptisation the agglomeration and aggregation between the particles in the sol-prepared powder is limited and the crystallite size is decreased from 10–50 nm to about 3 nm. As a result, the  $\text{BaSnO}_3$  powder obtained at  $330^\circ\text{C}$  shows a much larger specific surface area. During the thermal treatment of the sol-prepared powder, the dehydroxylation and dehydration of  $\text{BaSn}(\text{OH})_6$  begins at  $260^\circ\text{C}$  and ends at  $330^\circ\text{C}$ . As a result of the structure rearrangement at  $260^\circ\text{C}$ , the  $\text{BaSn}(\text{OH})_3$  phase transforms into an amorphous phase, from which the  $\text{BaSnO}_3$  phase nucleates and grows with an increase in temperature. This transformation is finished at  $330^\circ\text{C}$ . The sol-prepared powder is more sinter-active than the gel-prepared one. A  $\text{BaSnO}_3$  ceramic with a 90.7% theoretic density has been obtained by sintering the sol-prepared powder at  $1600^\circ\text{C}$  for 4 h.

#### References

1. Subbarao, E. C., Ceramic dielectrics for capacitors. *Ferroelectrics* 1981, **35**, 143–148.

2. Vivekanandan, R. and Kutty, T. R. N., Hydrothermal synthesis of Ba(Ti Sn)O<sub>3</sub> fine powders and dielectric properties of the corresponding ceramics. *Ceram. Int.* 1988, **14**, 207–216.
3. Wernicke, R., Influence of microstructure on the electrical properties of intergranular capacitors. *Ber. Dtsch. Keram. Ges.* 1978, **55**, 356–358.
4. Brauer, H., Grain-boundary barrier layers in Barium metatitanate ceramic with a high effective dielectric constant. *Z. Angew. Phys.* 1970, **29**, 282–287.
5. Moseley, P. T., Williams, D. E. and Tofield, B. C., Electrical conductivity and gas sensitivity of some transition metal tantalates. *Sens. Actuators* 1988, **14**, 79–91.
6. Moseley, P. T., Stoneham, A. M. and Williams, D. E., *Techniques and Mechanisms in Gas Sensing*. Adam Hilger, Bristol, 1991, Chapter 4.
7. Shimizu, Y., Shimabukuro, M., Arai, H. and Seiyama, T., Humidity-sensitive characteristics of lanthanum(3+)-doped and undoped strontium tin oxide (SrSnO<sub>3</sub>). *J. Electrochem. Soc.* 1989, **136**, 1206–1210.
8. Lumpe, U., Gerblinger, J. and Meixner, H., Carbon-monoxide sensors based on thin films of BaSnO<sub>3</sub>. *Sens. Actuators B* 1995, **24/25**, 657–660.
9. Lumpe, U., Gerblinger, J. and Meixner, H., Nitrogen oxide sensors based on thin films of BaSnO<sub>3</sub>. *Sens. Actuators B* 1995, **26/27**, 97–98.
10. Zhou, Z. and Zhao, G., BTS: a new ferroelectric for multifunctional sensors. *Ferroelectrics* 1990, **101**, 43–54.
11. Sano, H. and Herber, R. H., Moessbauer parameters of barium stannate. *J. Inorg. Nucl. Chem.* 1968, **30**, 409–413.
12. Wagner, G. and Binder, H., *Z. Anorg. Allegem. Chem.* 1958, **297**, 328–346.
13. Coffen, W. W., Ceramic and dielectric properties of the stannates. *J. Am. Ceram. Soc.* 1953, **367**, 207–214.
14. Savos'kina, A. I., Ya Goroshenko, G. and Selivanova, L. Ya., Synthesis of finely divided barium stannate (BaSnO<sub>3</sub>) from coprecipitation products (Russ.). *Izv. Akad. Nauk. SSSR Neorg Mater.* 1984, **203**, 472–475.
15. Licheron, M., Jouan, G. and Husson, E., Characterization of BaSnO<sub>3</sub> powder obtained by a modified sol-gel route. *J. Eur. Ceram. Soc.* 1997, **17**, 1453–1457.
16. Azad, A. M. and Hon, N. C., Characterization of BaSnO<sub>3</sub>-based ceramics. *J. Alloys Comp.* 1998, **270**, 95–106.
17. Udawatte, C. P., Kakihana, M. and Yoshimura, M., Preparation of pure perovskite-type BaSnO<sub>3</sub> powders by the polymerized complex method at reduced temperature. *Solid State Ionics* 1998, **108**, 23–30.
18. Kutty, T. R. N. and Vivekanandan, R., BaSnO<sub>3</sub> fine powders from hydrothermal preparation. *Mater. Res. Bull.* 1987, **22**, 1457–1465.
19. Dumanski, A., Kniga, A. and Kolloid Z., Die Weinsäuremethode zur Herstellung negativ geladener Sole. 1928, **44**, 273–277.
20. Dhar, N. R. and Varadanam, C. I., Preparation and properties of highly concentrated sols. Part V. Stannic hydroxide sols. *J. Indian Chem. Soc.* 1936, **13**, 602–608.
21. Scherrer, P., *Gött. Nachrichten*. Conference on July 26th, 1918, pp. 99–100.
22. Hollman, K. and Arnold F., *Lehrbuch der anorganischen Chemie*. Walter de Gruyter, Berlin, 1985.